Sensors and Materials, Vol. 37, No. 12 (2025) 5561–5576
MYU Tokyo

S & M 4263

Cooperative Control Strategy of Vehicle Motors Using Modified Quantum 3D Technology

Wen Cheng Pu* and Chi Hong Chen

Department of Electrical Engineering, National Chin-Yi University of Technology,
No. 57, Sec 2, Zhongshan Rd, Taiping Dist. Taichung 41170, Taiwan (ROC)

(Received June 5, 2025; accepted December 8, 2025)

Keywords: CAN, PIOT, power wave, Pu's count modulation, Mega2560

We propose a novel approach for constructing a Power Internet of Things (PIOT) collaborative network architecture using intelligent motors in this paper, eliminating the need for a traditional controller area network interface. The proposed system transforms the conventional centralized vehicle motor, call motor, control model—where a single control unit governs all motors—into a decentralized control framework. More importantly, it integrates modified quantum three-dimension (3D) communication (MQ3D), enabling coordination among different types (AC, DC) and quantities of motors through a smart DC bus architecture built with only two power lines. This configuration supports synchronized motor driving and improves system scalability. In conventional systems, motor operation can induce harmonic interference in control circuits due to fluctuating drive currents, potentially leading to malfunctions—especially when multiple heterogeneous motors operate simultaneously in complex harmonic environments. In contrast, the proposed system uses power waveforms as communication signals, avoiding the need for additional communication infrastructure, thereby reducing hardware costs. Moreover, unlike traditional communication platforms such as Wi-Fi or Bluetooth that rely on low-power signals susceptible to interference, power-based communication inherently offers greater noise immunity owing to its higher energy signals. The MQ3D technology applied in this study is a novel quantum communication method that does not require sidebands between communication channels and can operate at ultralow frequencies (below 1 Hz). The proposed method also addresses limitations in MQ3D's original amplitude-restricted design, which constrained data space and reduced communication speed. Effective motor collaboration requires not only responsive control units but also high-speed and reliable communication. To address the aforementioned issues, we also propose a PIOT system, implemented on an automotive platform using a smart motor architecture. Leveraging advances in quantum communication, we enhanced data throughput and the responsiveness of the motor collaboration system. To validate the proposed methodology, a test platform was developed using a personal computer, a custom smart DC bus controller, Arduino Mega2560, and various motors. MATLAB®, a packet software program, was employed for experimental verification, and the feasibility and correctness of the theoretical concepts proposed in this research were demonstrated.

*Corresponding author: e-mail: puo@ncut.edu.tw
https://doi.org/10.18494/SAM5775

ISSN 0914-4935
https://myukk.org/

1. Research Background

Traditional automotive actuators are primarily driven by DC motors, which are directly controlled by controllers, as illustrated in Fig. 1. In many cases, a controller area network (CAN) interface is used to establish a local network for signal transmission.[1–3] As shown in recent literature, the CAN interface has been widely used in smart vehicle control applications. Among them, Hanzálek *et al.* [1] utilized CAN for autonomous driving trajectory control, whereas Gao *et al.*[2] investigated the automation of intelligent vehicles, focusing on the protection mechanisms of the system under denial of service attacks. Aljabri *et al.*[3] described the implementation of the CAN system within intelligent vehicles and the use of vehicle-to-everything (V2X) technology to establish network communication outside the vehicle, studying how to prevent security issues caused by network hacking during autonomous driving. The CAN interface, developed by Bosch Company, is widely utilized in automotive equipment networks, industrial instrumentation, medical devices, HVAC systems, elevators, and other automation-related communication applications. It has been standardized through ISO 11898 and ISO 11519. At the physical layer, the CAN interface requires only two communication wires, making it a low-power communication platform. It adopts a two-wire differential signal transmission method. Even if one of the differential bus signal lines is disconnected, grounded, or shorted to a power line, the system can continue to transmit signals. This makes CAN the most commonly used communication platform in automotive electronics today. It uses an electrical signal of 2.5 V ± ΔV to transmit a single bit of data, where CAN_H and CAN_L respectively represent digital signals '1' and '0'. The voltage difference ΔV is 2 V.[2,3] Owing to its small noise margin and low signal power, it is susceptible to noise from high-power load switching or environmental interference, which can cause malfunction. In recent years, academia has been exploring the application of quantum mechanics in computing, aiming to vastly surpass the computational capabilities of traditional computers. It redefines the data format using quantum bits (QBs), which differ from classical bits. QBs use the Bra-Ket notation to represent notations $|0\rangle$ and $|1\rangle$ to replace binaries 0 and 1, respectively. While classical bits can only represent one of two values at

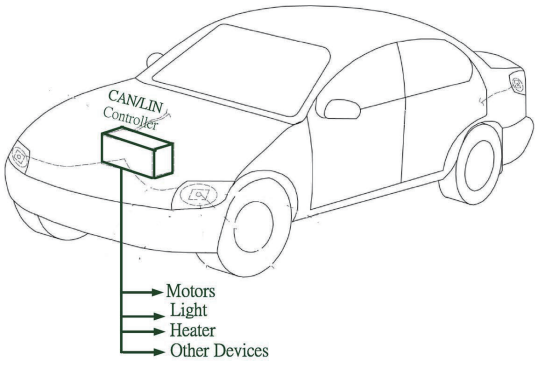

Fig. 1. Traditional automotive motor drive system.

a time, QBs can exist in a superposition of both |0⟩ and |1⟩, forming a data space that can be represented as a plane, allowing two bits of information to be transmitted simultaneously, doubling the transmission speed. In other words, if an n-dimensional feature space is constructed, it would be possible to transmit n data streams simultaneously, effectively increasing communication speed by a factor of n. However, owing to the limitations in our understanding of the microscopic world, measuring quantum states can introduce load effects that collapse the quantum state, impacting the accuracy of computations. As a result, the quantum trajectory described by the wave function can only be represented probabilistically through repeated measurement and is used to achieve the benefits of rapid computation. According to the literature, many quantum computing systems are applied in various fields such as quantum computers, quantum networks, TUM cryptography, and quantum machine learning.[4] The goal is to increase execution speed.[4–12] However, apart from the collapse problem, multiple measurements are required to obtain the probabilities of different quantum states. For nonspecific problems, the execution speed may not necessarily be higher than that of traditional binary computers. Moreover, although the literature discusses hardware issues,[4] most of the focus is on algorithms and processes.[4,9] Among them, Ganguly *et al.*[5] explored the data security issues of quantum bits during communication, introducing the concept of blockchain into quantum communication technology and proposing a new quantum secure direct communication (QSDC) method, i.e., "we conceive QSDC-based blockchain for identity verification, message encryption, and consensus". Yang *et al.*[6] investigated the application of quantum entanglement theory in the Internet of Things (IoT) for bidirectional communication. Sun *et al.*[7] used quantum and mobile edge computing (MEC) to optimize sixth-generation (6G) wireless networks. Jiang *et al.*[8] explored quantum computer architectures that differ from the von Neumann architecture. Huynh *et al.*[9] leveraged the capabilities of quantum computing to optimize power systems. However, the physical properties of quantum systems inherently make them susceptible to noise and quantum coherence, increasing the probability of errors.[4,9] Although quantum devices have been extensively studied recently, they all require new hardware setups and incur significant costs, making them inaccessible to the general public.[4] Therefore, in this study, we propose simulating quantum mechanics principles on traditional binary computers to create a binary computer with quantum bit functionality (referred to as a quantum computer). This approach reduces hardware costs and, through an algorithm that transmits 3D spatial data using two components, increases communication bandwidth. Additionally, it enables quantum computers interconnected in the Power Internet of Things (PIOT) network to be compatible with different data lengths and to have high noise resistance.[13–15] Finally, each quantum computer will serve as an interface for the motor in the automotive power system and will be responsible for encapsulating the motor into a new motor type, called a smart motor. In this architecture, heterogeneous motors are encapsulated within it, and the operator only needs to give commands to the quantum computer without needing to know how the motors operate. The architecture can also encapsulate other electrical loads in the car, thereby simplifying the complexity of the motor drive.

2. Research Methodology

To address the aforementioned issues, we first propose a PIOT system, implemented on an automotive platform using a smart motor architecture. This motor drive system operates over a smart DC bus composed of only two power lines, which simultaneously deliver power to drive the motor and transmit communication data.

The smart motor architecture, as shown in Fig. 2, consists of a control unit and a motor unit. Regardless of whether the internal motor is AC or DC, the control unit encapsulates it as a single module. Although different types of motor require different driving methods, this is handled entirely by the control unit. The operator does not need to understand the specific motor type or control method, and commands are simply issued via the power lines. This considerably simplifies the user's operation process. Figure 3 shows how a PIOT network can be easily constructed using the smart DC bus in power lines. The smart DC bus is different from the traditional DC bus, which only supported power as it simultaneously delivers both motor-driving power and communication capability. This PIOT system will serve as the test platform in this research.

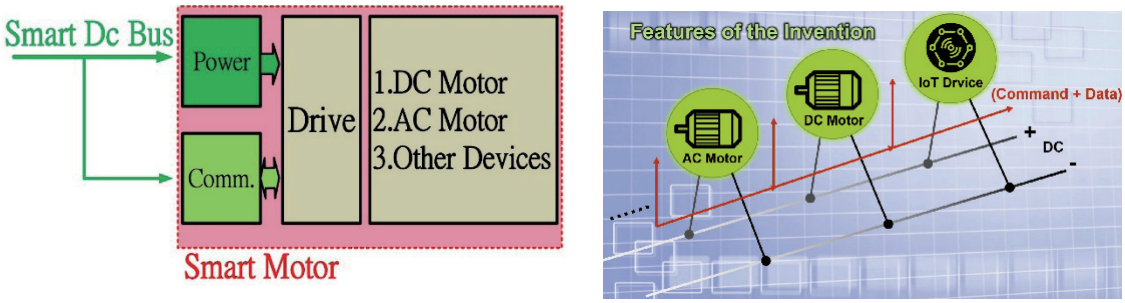

(a) (b)

Fig. 2. (Color online) Smart motor: (a) architecture and (b) application.

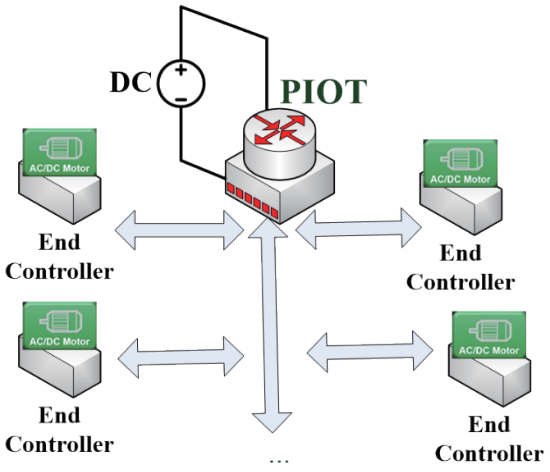

Fig. 3. (Color online) Architecture of PIOT.

The PIOT utilizes pu's count (PK) modulation (PK modulation, PKM) to encode data into power waves, aiming to support packets of any length and transmission speed, while enhancing noise immunity.[13–15] The PK encoding process is shown in Fig. 4, and the encoded number of pulses, N, can be calculated as

$$N = \left(\text{Value of bit} + 1\right) * 2^{\gamma} + 2^{\gamma-1},\ \gamma = \text{Error Level Coefficient}. \tag{1}$$

After PKM, the data becomes a sequence of power wave pulses.[13–15] For example, if the communication environment parameter $\gamma = 3$, N can be easily calculated using Eq. (1). Depending on the bit value,

$$N = \begin{bmatrix} 12 & 20 & 28 \end{bmatrix} \times D. \tag{2}$$

As shown, if we choose 3 in accordance with the communication environment, the above equation can be transformed into Eq. (2) when the bit data is '0', $D = [1\ \ 0\ \ 0]^{-1}$, when the bit data is '1', $D = [0\ \ 1\ \ 0]^{-1}$, and when the bit data is the end bit, $D = [0\ \ 0\ \ 1]^{-1}$. In the physical layer of PIOT network communication, the difference voltage ΔV representing the digital signals '1' and '0' in the physical layer is twice the power signal. In other words, when the power system uses 12 V in the vehicle, ΔV is 24 V compared with 2 V for CAN.[2] The communication interference will arise when one of the vehicle motors or other electrical loads is turn on or off in the vehicle, and the instantaneous large current will induce an electrical voltage in the communication line. The external environmental signal interference also has a greater noise resistance capability.

Most importantly, establishing a CAN communication platform additionally increases system costs. Moreover, in recent years, quantum computers have been widely discussed because traditional computers can also significantly increase computing speed through quantum computing methods. However, the hardware and costs are substantial, and the real solution must incorporate probabilities to predict results, making it unsuitable as a general-purpose computer

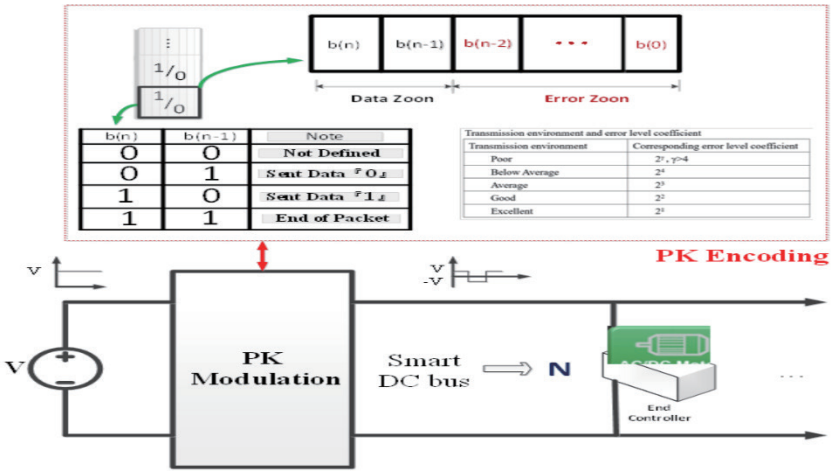

Fig. 4. (Color online) PKM encoding process.

for solving various problems. The main research objective described in this paper is to increase the communication speed of PIOT. Therefore, we reference the superposition characteristic of quantum computers, allowing the transmitted data to be presented in a parallel communication manner and simulating the entanglement characteristic of quantum mechanics to transmit to another endpoint. The former references the electrons (Q_1, Q_2, …, Q_n) orbiting a proton in a microscopic quantum space, as shown in Fig. 5. Each operating electron maintains a fixed posture in space, running in a rotational or fixed mode. In this study, we simulated the posture of electrons in space, while each electron's posture in 3D quantum space serves as components for the data to be transmitted. In other words, a single electron in 3D quantum space can transmit three pieces of data simultaneously. If n electrons are transmitted at the same time, it can send $3n$ pieces of data. However, the method proposed in the literature[14,15] can only utilize the posture component data of a two-dimension (2D) plane, failing to realize the actual transmission of 3D spatial posture components, indicating that traditional methods can transmit, at most, $(2n + 1)$ pieces of data simultaneously.

In this research, we propose a correction method that still utilizes two-axis components but can transmit three-axis data in 3D space to increase the data volume in PIOT network communication. Relevant inferences will be explained in the next section.

Additionally, this study is based on a system built on the PIOT network, primarily focusing on how to increase communication bandwidth. Since quantum communication is a potential solution, we mainly explore applications for increasing data transmission. Referring to the quantum spatial system, as shown in Fig. 5, electrons (Q_1, Q_2, …, Q_n) in a steady state orbit the atomic nucleus at a fixed angular velocity ω, and each electron has a different posture, indicating that each electron has different components in 3D space. Referring to Fig. 6, we let λ represent the interaction of the electron with the atomic nucleus; then, the components in the 3D

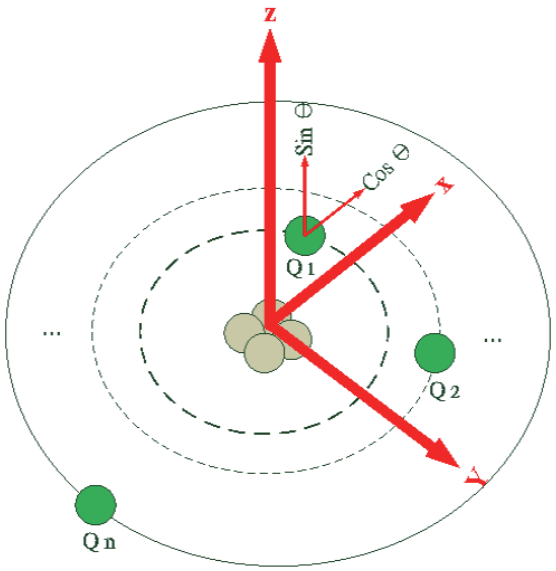

Fig. 5. (Color online) MQ3D quantum simulation space.

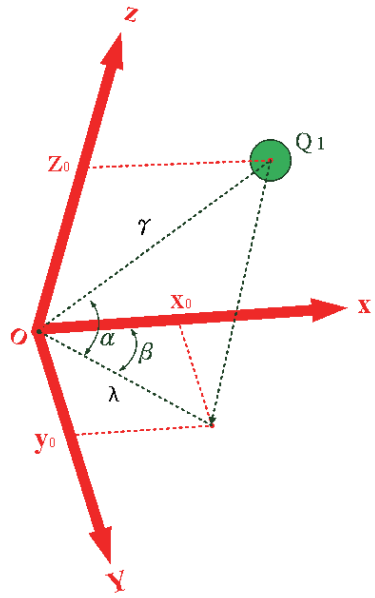

Fig. 6. (Color online) Relationships between quantum space components.

dimensions can be calculated as shown in Eq. (1), where α and β represent the angles of the electron's projection in the X–Y plane and with respect to the Z-axis, respectively.

$$\begin{bmatrix} x_0 \\ y_0 \\ z_0 \end{bmatrix} = \lambda \begin{bmatrix} \cos\beta & 0 & 0 \\ 0 & \sin\beta & 0 \\ 0 & 0 & 1 \end{bmatrix} \begin{bmatrix} \cos\alpha & 0 & 0 \\ 0 & \cos\alpha & 0 \\ 0 & 0 & \sin\alpha \end{bmatrix} \begin{bmatrix} 1 \\ 1 \\ 1 \end{bmatrix} \tag{3}$$

In this context, a single electron in 3D can simultaneously carry three components of data, but the question is how to transmit this data. According to Refs. 13–15, within a communication frequency, orthogonal sine and cosine functions can be decomposed into two communication channels in two dimensions to transmit bit data. However, this method utilizes multiple communication frequencies ($f_1, f_2,\ldots f_n$) to carry two components of bit data (D_0, D_1, $D_2,\ldots,D_n$), as shown in Eq. (2). Although this method is simpler, each communication frequency can only transmit 2D plane component data, allowing for the transmission of ($2n$ + 1) bits of data at a time.

$$f(t) = D_0 + D_1\cos 2\pi f_1 t + D_2\sin 2\pi f_1 t + \cdots + D_{2n-1}\cos 2\pi f_n t + D_{2n}\sin 2\pi f_n t \tag{4}$$

To increase the transmission of 3D component data and enhance communication bandwidth, we combined component data quantization and polarization techniques to transmit 3D component data in a 2D mode. To achieve this goal, we no longer transmitted digital signals; instead, the data was transmitted as analog signals A_i after being converted from digital data via D/A conversion, where ρ represents the resolution of the analog signal conversion from the number of digital data bits, n. Upon receiving this analog signal, the receiving end will convert it back into

a digital signal by A/D conversion. The number of bits for quantization is determined using Eq. (5), ensuring that as long as the resolution ρ is greater than the maximum error ε during the restoration at the receiving end, the signal can be restored. In other words, a component that originally can only transmit one bit of data can now transmit n bits of data, thereby increasing the communication bandwidth by n times.

$$\rho = \frac{A_i}{2^n} \tag{5}$$

$$\rho > \varepsilon \tag{6}$$

Furthermore, according to the diagram shown in Fig. 6, the distance from Q_1 to the origin O is Υ and the angle with the X–Y plane is α. Additionally, λ is the length of the projection of Υ onto the X–Y plane. On the basis of the geometric structure, the components of Q_1 along the X- and Y-axes can be derived from Υ and β. Similarly, the component along the Z-axis can be determined from Υ and α. Using the principles of trigonometry, the component along the z-axis can be determined from the hypotenuse and the included angle. Additionally, the information being transmitted can be inferred from Eq. (3). Thus, we only need two pieces of polar coordinate data, distance and angle, to determine any point in 3D space. Moreover, as shown in Fig. 7, the quantized distance data is filled into region (I) and the quantized angle data is filled into region (II). The resulting data after filling in is as shown in Fig. 7, and then, the amplitude component is calculated as

$$M = (\text{Data})_{10} * \rho\,, \tag{7}$$

where $(\text{Data})_{10}$ indicates the corresponding decimal value. Another advantage of PK encoding is that it inherently includes a synchronization signal. As illustrated, regardless of whether the transmitted bit data is '0', '1', or an end bit, the encoded data becomes a series of pulse waves, as shown in Fig. 8. We can easily extract the low-frequency wave at its edges, allowing for synchronized data transmission between the receiving and transmitting ends, independent of the pulse wave speed. In other words, the receiving end can simply count the number of pulses between synchronization pulses to restore one bit of data.

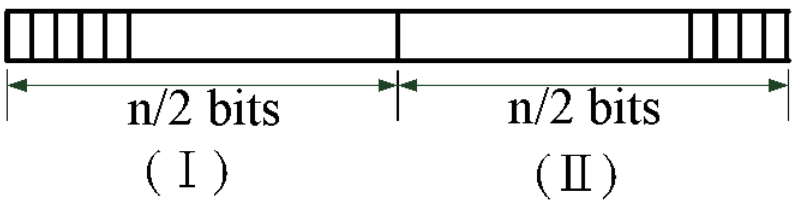

Fig. 7. Format of A/D after quantification.

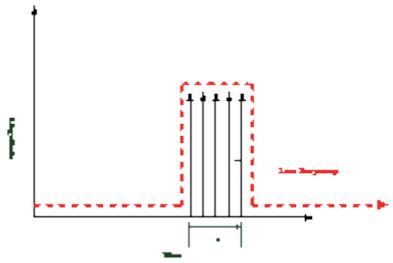

Fig. 8. (Color online) The synchronization signal is hidden in this sequence wave.

PK encoding technology can also tolerate noise interference during the communication process. Each bit of data is received one by one, and it includes an end bit, allowing the receiving end to clearly determine, at any time, that the transmission process has concluded. Therefore, it can transmit data of any length. After receiving the data, the receiving end calculates each component's data according to Eqs. (1) to (9). Since each component represents a piece of transmitted data, while traditional methods can only transmit two components of data, we can transmit three components of data, resulting in a total data transmission of $(3n + 1)$ times.

$$\gamma = \sqrt{x_0^2 + y_0^2 + z_0^2} \tag{8}$$

$$\alpha = \tan^{-1}\left(\frac{y_0}{x_0}\right) \tag{9}$$

$$\beta = \sin^{-1}\left(\frac{z_0}{\gamma}\right) \tag{10}$$

According to Fourier's theory, every periodic wave is composed of waveforms at multiples of its frequency, so signals at these different frequencies can be used as channels for communication. At the same time, each communication frequency can be divided into two independent components, COS and SIN, so each frequency can be split into two communication channels; then, we can rearrange Eq. (1) into the following matrix form:

$$\begin{aligned} f(t) &= A_0 + A_1 \cos 2\pi f_1 t + A_2 \sin 2\pi f_1 t + \ldots + A_{2n-1} \cos 2\pi f_n t + A_{2n} \sin 2\pi f_n t \\ &= W_0 + W_1 \cos 2\pi f_1 t + W_2 \sin 2\pi f_1 t + \ldots + W_{2n-1} \cos 2\pi f_n t + W_{2n} \sin 2\pi f_n t \\ &= \begin{bmatrix} W_0 & W_1 & \ldots & W_{2n} \end{bmatrix} \begin{bmatrix} G_0 \\ \ldots \\ G_{2n} \end{bmatrix}, \end{aligned} \tag{11}$$

where

A_i is the analog signal of the i th communication channel,
$W_i = A_i$,
$G_{2i-1} = \cos(i \cdot 2\pi f_1 t)$,
$G_{2i} = \sin(i \cdot 2\pi f_1 t)$,
$i = 1, 2, 3, \ldots, n$.

Thus, after changing the digital signal D_i shown in Eq. (2) to an analog signal A_i, only two pieces of data are needed to send this signal to the transmission medium, while the receiving end processes it in reverse to restore each component's data, completing the communication process. According to the principle, if a matrix is used for solving, to find m unknowns, M sampling points must be collected. However, as the dimensions of the quantum space increase, the number of sampling points becomes very large, resulting in a massive matrix calculation. Therefore, we employed neural networks for computation, wherein the dimensions increase in a linear manner, thereby increasing the number of computational steps without causing excessive complexity as in matrix methods. The receiving end utilizes a neural network to extract the structure of each component's data, thus creating a larger data transmission space. In any case, the role of the neural network is to classify the input data by determining factor η, and the receiver in this study adopts the architecture of the neural network shown in Fig. 9 and converges the weight W using Eq. (12).[15]

$$W = \begin{bmatrix} W_0 & \ldots & W_{2i} \end{bmatrix}, \quad i = 1, 2, 3, \ldots, n$$
$$W^T(t+1) = W^T(t) + \Delta W^T = W^T(t) + \eta(f - \hat{f}) \begin{bmatrix} G_0 \\ \ldots \\ G_{2n} \end{bmatrix} \tag{12}$$

The transmission and reception processes are shown in Figs. 10 and 11, respectively.

Finally, combined with the neural network and MQ3D algorithm, the power system of the vehicle becomes a PIOT network that can be controlled decentrally, and the system structure proposed in this study is shown in Fig. 12.

3. Implementation and Verification

The architecture of the motor collaboration system is shown in Fig. 13, and the quantum communication architecture proposed in this study primarily focuses on constructing the dimensional components of a quantum 3D space using two datasets from the MQ3D. This approach aims to enhance communication speed within the PIOT network. The system simulation platform is implemented using the MATLAB® software suite on a PC. At the start of the simulation, a continuous spectrum ranging from f_1 = 0 to 30 Hz is selected to simulate the

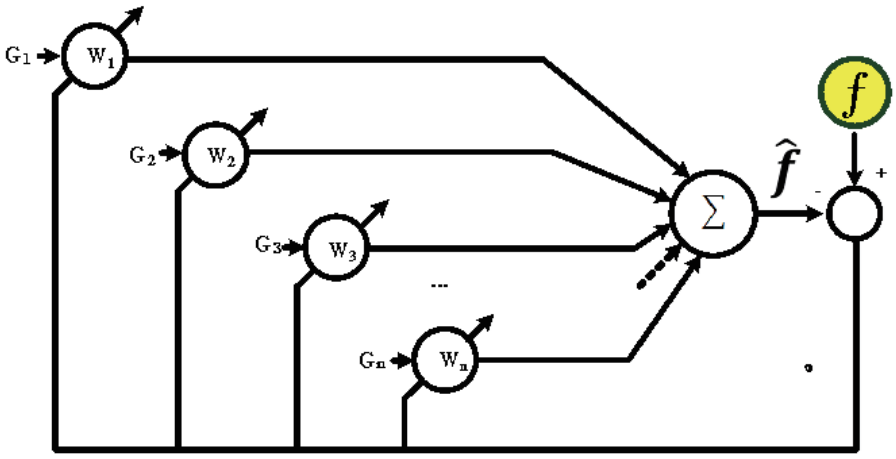

Fig. 9. (Color online) This diagram shows that the receiver uses a neural network to extract a component data structure.

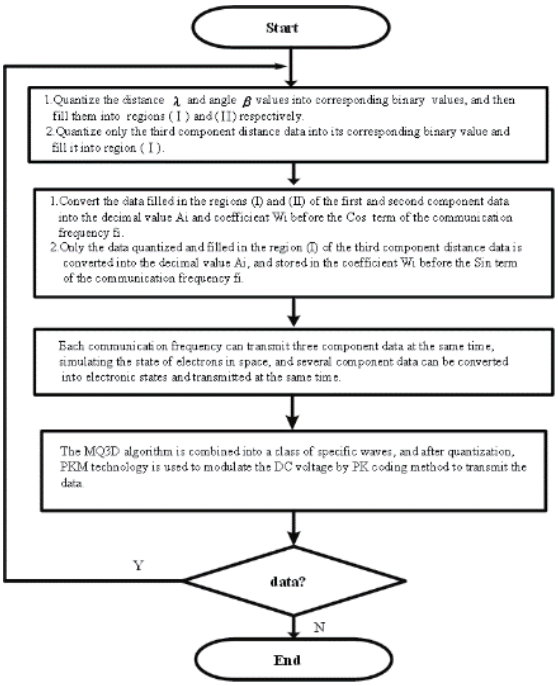

Fig. 10. MQ3D transmission process.

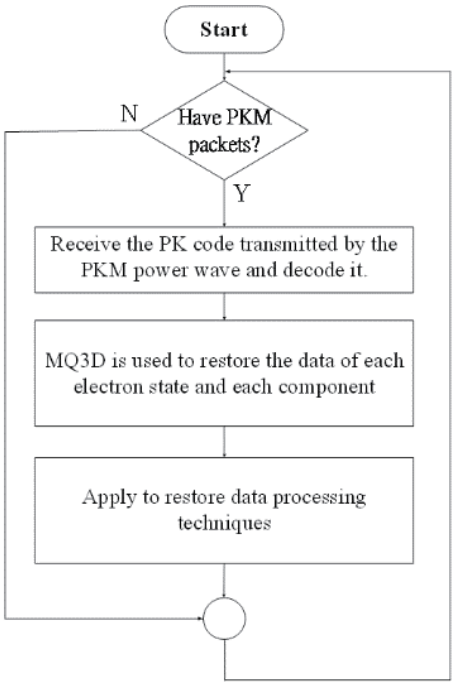

Fig. 11. MQ3D receiving process.

architecture of a quantum bit with 61 communication channels. Each channel is equipped with 16-bit data. Therefore, at an extremely low carrier frequency (0–30 Hz), the system can get a lot data, 2 (byte) × 61 (channel) × 1 (Cycle) × 360/60 = 732 (bytes), per cycle. In the experiment, following the architecture depicted in Fig. 8 and the transformation methods described in Eqs. (6) and (10), the transmitter modulates the digital data to be transmitted into analog data, incorporating the weight W values given below. This data is then transmitted via the carrier

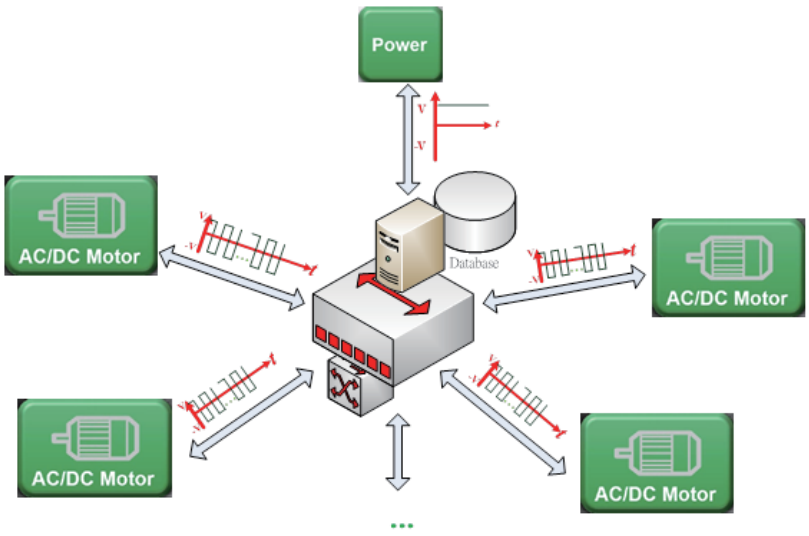

Fig. 12. (Color online) System structure proposed in this study.

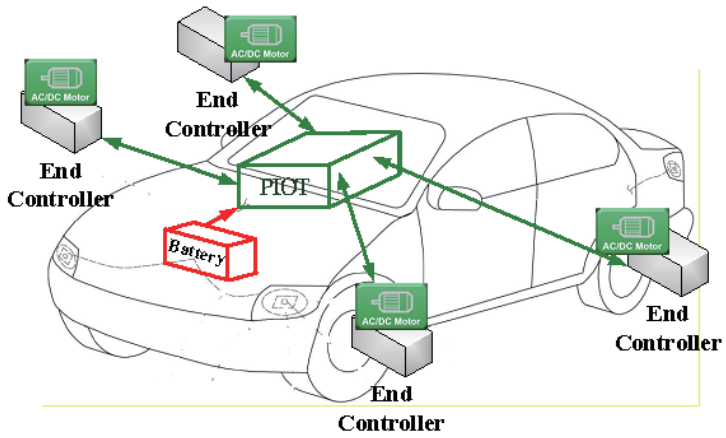

Fig. 13. (Color online) Architecture of motor collaboration system.

channels. If the data transmission is zero except for the specified components, the receiver, after capturing the data, processes it as shown in Fig. 14.

$$\begin{aligned} w(1) &= 1.05 \\ w(2) &= 1.0 \\ w(3) &= 1.0 \\ w(4) &= 1.0 \\ w(5) &= 1.0 \\ w(7) &= 1.0 \end{aligned} \tag{13}$$

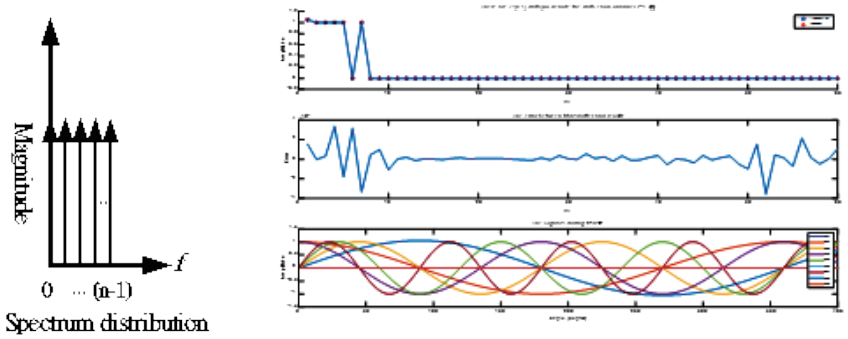

(a) (b)

Fig. 14. (Color online) Process of MQ3D: (a) spectrum distribution and (b) process wave.

The process of restoring the analog values is then calculated separately. Figure 6 shows that the analog data received by the receiver has an error margin of $\pm 10^{-8}$ compared with the data transmitted by the transmitter. Given a 16-bit resolution (1/65535), it can be concluded that the receiver accurately restores the data transmitted by the transmitter. The top graph in Fig. 14 shows the actual simulation results of the communication between the two ends, while the bottom graph shows the waveforms of each communication channel during the simulation. Figures 15 and 16 demonstrate that the small and tiny analog signals are transmitted by the transmitter, as shown in Eq. (12), and the receiver can accurately parse and restore them. Figure 15 shows that, after incorporating the weight W from Eq. (13), the error margin between the restored values at the receiver changes from $\pm 10^{-9}$ to $\pm 10^{-10}$. In other words, as shown in Fig. 17, Value_x represents the amplitude of the analog signal calculated using a lower resolution from Eq. (6), while Value_y represents the data restored by the receiver.

$$\begin{aligned} w(1) &= 0.05 \\ w(3) &= 0.03 \\ w(5) &= 0.02 \\ w(7) &= 0.04 \\ w(8) &= 0.1 \end{aligned} \tag{14}$$

$$\begin{aligned} w(1) &= 0.005 \\ w(3) &= 0.003 \\ w(5) &= 0.002 \\ w(7) &= 0.004 \\ w(8) &= 0.001 \end{aligned} \tag{15}$$

Figures 15 and 16 show the feasibility of the method proposed in this paper, and the data also prove that the lower the resolution, the higher the accuracy of the signal restored at the receiver, as shown in Fig. 17.

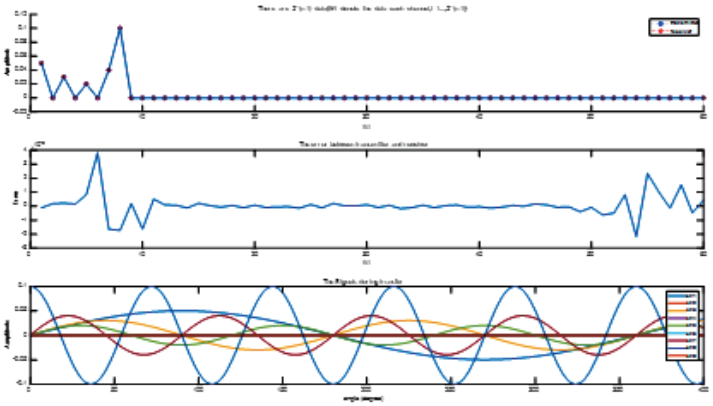

Fig. 15. (Color online) MQ3D of small signal analysis.

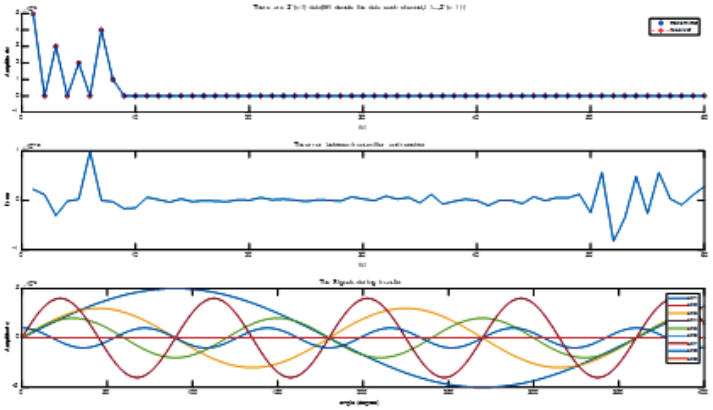

Fig. 16. (Color online) MQ3D resolution of tiny signals.

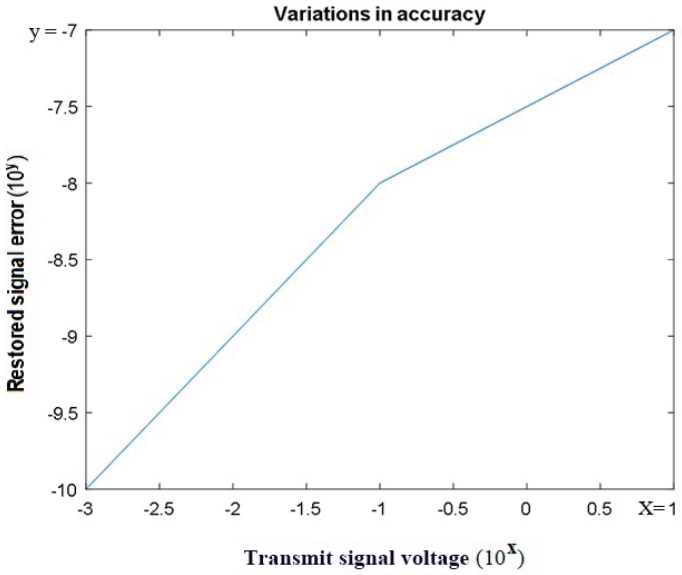

Fig. 17. (Color online) Effect of restored signal in MQ3D.

The implementation platform of this study is shown in Fig. 18. Before implementation, the resolution ρ is set to ensure that both communication parties can utilize it. Subsequently, the transmitter, following the method depicted in Fig. 8, converts digital commands into analog signals using the weight W through D/A conversion. These signals are then quantized into digital data and directly modulated into a sequence of power waves via PKM. The power waves are broadcast through the smart bus to the smart motors connected to the PIOT network. Each smart motor decodes the signals using PK, receives the complete digital data, and multiplies it by the resolution ρ to obtain the corresponding analog data. The receiver simulates the process of sampling the analog signal once. On the basis of Eq. (11), the analog weight data carried by the 61 communication channels is restored, divided by the resolution ρ and converted back into the digital structure shown in Fig. 8. Additionally, the 3D component values representing the motion are derived by reversing Eqs. (8) to (10). In the experiment, a random digital command is transmitted 10 times to control the activation of a specific motor as one experimental cycle. This process is repeated four times, and the actual activation count is recorded and statistically analyzed. Figure 19 shows the results.

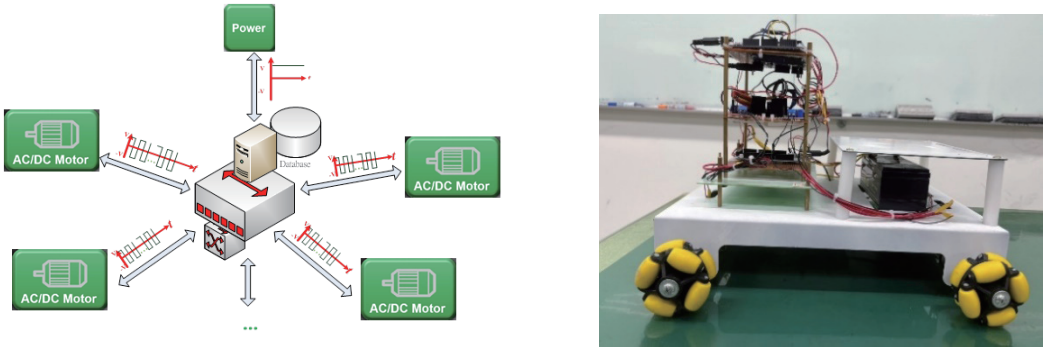

(a) (b)

Fig. 18. (Color online) Implementation system: (a) architecture diagram and (b) entity photograph.

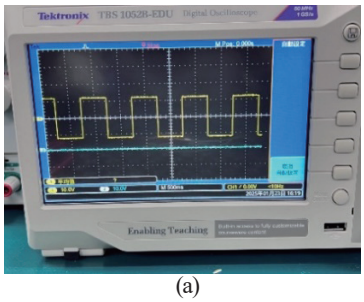

(a)

Digital commands in transmitter	Accurate times
Smart motor 1	10
Smart motor 4	10
Smart motor 1	10
Smart motor 3	10

(b)

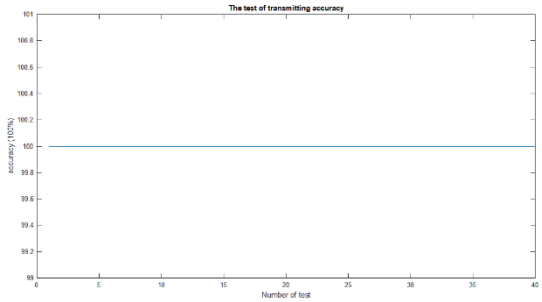

(c)

Fig. 19. (Color online) Experimental results: (a) PIOT waveform, (b) experimental data, and (c) accuracy.

4. Conclusions

In this study, we proposed a quantum communication algorithm that simulates the quantum characteristics of superposition in communication. Many transmitted bits can be sent at the same time, which increases the data speed compared with the traditional digital one whose data transmission speed was just one bit at a time, and two sets of analog data are used to represent the components of three axes, thereby enhancing the communication bandwidth of quantum communication technology. This is the most significant contribution of this research. Additionally, integrating smart motors with the PIOT system enables the control of all vehicle motors and even loads in a vehicle using just one set of DC power lines. This simplifies the vehicle's power system and driving mechanisms. Our approach eliminates the need for specialized communication equipment, addresses the issue of CAN bus signal gaps being too narrow and prone to interference, and improves the reliability of communication signals by defining bit data on the basis of power levels. This is another key contribution of this study. Such applications can be extended to any electrical system in the future, establishing higher bandwidth and more efficient automated systems.

References

1 Z. Hanzálek, J. Záhora, and M. Sojka: IEEE J. Vehicu. Techn. **1** (2024) 362. https://doi.org/10.1109/TVT.2023.3309554.
2 S. Gao, L. Zhang, L. He, X. Deng, H. Yin, and H. Zhang: IEEE J. Vehicu. Techn. **1** (2023) 16624. https://doi.org/10.1109/TVT.2023.3296705.
3 W. Aljabri, Md. A. Hamid, and R. Mosli: IEEE Intell. Transp. Syst. Mag. **2** (2025) 2282. https://doi.org/10.1109/TITS.2024.3509459.
4 A. Mondal and K. K. Parhi: IEEE Circuits Syst. Mag. **1** (2024) 33. https://doi.org/10.1109/MCAS.2024.3349668.
5 A. Ganguly, S. Abadal, I. Thakkar, N. E. Jerger, M. Riedel, M. Babaie, R. Balasubramonian, A. Sebastian, S. Pasricha, and B. Taskin: IEEE Micro **2** (2022) 40. https://doi.org/10.1109/MM.2022.3150684
6 Z. Yang, M. Zolanvari, and R. Jain: IEEE Commun. Surv. Tutors. **25** (2023) 1059. https://doi.org/10.1109/COMST.2023.3254481.
7 Z. Z. Sun, Y. B. Cheng, M. Wang, L. Qian, D. Ruan, D. Pan, and G. L. Long: IEEE Internet Things J. **12** (2025) 14375. https://doi.org/10.1109/JIOT.2025.3526443.
8 J. L. Jiang, M. X. Luo, and S. Y. Ma: IEEE J. Sel. Areas Commun. **42** (2024) 1900. https://doi.org/10.1109/JSAC.2024.3380091.
9 D. V. Huynh, O. A. Dobre, and T. Q. Duong: IEEE Commun. Lett. **29** (2025) 448. https://doi.org/10.1109/LCOMM.2024.3523421.
10 Zebo Yang, Maede Zolanvari, Raj Jain: IEEE Commun. Surv. Tutors. **25** (2023) 1059. https://doi.org/10.1109/COMST.2023.3254481.
11 M. A. Shafique, A. Munir, and I. Latif: IEEE Access **12** (2024) 22296. https://doi.org/10.1109/ACCESS.2024.3362955.
12 Y. Zhou, Z. Tang, N. Nikmehr, P. Babahajiani, F. Feng, T. C. Wei, H. H. Zheng, and P. Zhang: iEnergy **1** (2022) 170. https://doi.org/10.23919/IEN.2022.0021.
13 W. C. Pu, Y. D. Lin, and K. H. Chao: Sens. Mater. **35** (2023) 2035. https://doi.org/10.18494/SAM4068.
14 W. C. Pu, Y. D. Lin, and J. X. Wu: Sens. Mater. **32** (2020) 1865. https://doi.org/10.18494/SAM.2020.2488.
15 W. C. Pu, Y. D. Lin, and K. H. Chao: Sens. Mater. **31** (2019) 4029. https://doi.org/10.18494/SAM.2019.2379.